КОНДЕНСАЦИЯЛАНҒАН КҮЙДІҢ ФИЗИКАСЫ
ФИЗИКА КОНДЕНСИРОВАННОГО СОСТОЯНИЯ
PHYSICS OF THE CONDENSED MATTER

DOI 10.31489/2023PH2/6-16

UDC 666.3.016:537.226.1

A.V. Pavlov[1], A.M. Zhilkashinova[2], S.S. Gert[3], N.M. Magazov[4*], Zh.S. Turar[5], A.B. Nabioldina[6]

[1] Ceramic plant LLP "KAZ CERAMICS", Ust-Kamenogorsk, Kazakhstan;
[2,4,5,6] S. Amanzholov East Kazakhstan University, Ust-Kamenogorsk, Kazakhstan;
[3,4] D. Serikbayev East Kazakhstan Technical University, Ust-Kamenogorsk, Kazakhstan
([*]E-mail: magazovn@gmail.com)

Study of electrophysical properties of beryllium ceramics with the addition of micro- and nanoparticles of titanium dioxide

In the present paper the research results of influence of nanoparticles TiO_2 additions in the range 0,1 — 2,0 wt. % on electrophysical properties of oxide-beryllium ceramics ($BeO + TiO_2$) made of micropowders are presented. The electrophysical characteristics of synthesized ceramics modified with 30 wt. % TiO_2 micro- and nanoparticles in the electric current frequency range of 100 Hz — 100 MHz were studied by the total complex resistance method (impedance). It is known that the introduction of TiO_2 addition to the BeO-ceramics after heat treatment in a reducing atmosphere is accompanied by a significant increase in electrical conductivity and the ability to absorb electromagnetic radiation in a wide range of frequencies. According to the results of the studies it was found that the addition of nanoparticles TiO_2 into the ($BeO + TiO_2$)-ceramics significantly reduces its static electrical resistance in comparison with the serial sample, and the specific conductivity of such ceramics significantly increases at high frequencies ~ 10^7 Hz. The addition of TiO_2 nanoparticles significantly increases the dielectric losses of the sample sintered in the temperature range 1530 — 1550 °C. The values of real and imaginary parts of dielectric permittivity of such ceramics and the tangent of the angle of dielectric loss are two times higher compared to the serial sample — BT-30 (B — beryllium, T — titanium). The obtained results are unique in their kind, due to the experiment with a rare and strategically important material — beryllium oxide and the possibility of synthesizing new nanostructures based on it.

Keywords: dielectric permittivity, conductivity, electric current frequency, impedance, nanoparticles, beryllium oxide, titanium dioxide.

Introduction

Currently, industrial progress requires electronics to continuously increase the level of power, efficiency, reliability and durability [1]. For modern devices, in particular powerful RF (radio frequency) and SHF (super high frequency) transmitters, power transistors, power converters, reliability under conditions of high currents and high temperatures is certainly a key factor [2]. Also, ceramic materials, often used to replace metals and alloys, have not only heat resistance and high strength, but also special electrophysical properties [3, 4], which contributes to their wide use in electronic engineering [5]. Such ceramics include beryllium oxide, the effective component of dielectric permittivity of which is 6.9 — 7.5, the tangent of angle of dielectric losses $tg\delta = 3 \cdot 10^{-4}$ at frequency f = 1 MHz [6]. BeO-ceramic is a material of super refractory class, which in addition to dielectric properties is characterized by high vacuum density, mechanical strength, thermal conductivity, thermal stability and heat resistance. The unique combination of physical and chemical properties of beryllium oxide (BeO) [7] determines a wide range of BeO-ceramics use in various fields of modern technology and special instrumentation [8]. High radiation resistance [9], thermal conductivity [10], dielectric strength and transparency to X-ray, ultraviolet radiation, visible IR (infrared) and SHF radiation

[11] make BeO-ceramics the most promising material for use in various devices of electronic engineering of responsible purpose [12]. Along with high thermal conductivity — 280 — 320 W/(m·K), pure BeO-ceramics have high electrical resistance (~$1 \cdot 10^{15}$ Ohm cm at 300 K) [13]. This makes it possible to use BeO-ceramics in high-power resistors, transistors and microcircuits as highly efficient dielectric substrates for creating electronic devices and resonator tubes for gas OQG (optical quantum generator) and much more. Thermal conductivity of the BeO-ceramic is comparable with that of metals and is second only to diamond. The thermal conductivity of BeO ceramics can reach values from 300 to 320 W/(m·K), which is comparable with that of chemically pure copper, which has a thermal conductivity of ~ 400 W/(m·K) [14]. The specific electrical resistance of beryllium oxide ceramic samples at room temperature is in the range from 10^{14} to 10^{15} Ohm·cm. BeO-ceramic is a transparent material for vacuum ultraviolet (VUV), X-ray and super-high frequency (SHF) radiation [15]. In turn, the presence of developed interfaces and intergranular interactions can significantly affect the physicochemical and performance characteristics of the composite ceramics based on BeO. One of such additives capable of essentially changing the conducting and other properties of the BeO-ceramics is TiO_2 [16]. It is known that the addition of TiO_2 to the BeO-ceramics after heat treatment in a reducing atmosphere is accompanied by a significant increase in electrical conductivity and the ability to absorb electromagnetic radiation in a wide range of frequencies [17]. The different ratio in the BeO-ceramics of the TiO_2 component and the degree of its reduction allow to regulate the magnitude of electromagnetic wave absorption by such ceramics. At present, the most effective material with the ability to absorb electromagnetic waves is the composition of BeO + 30 wt % TiO_2. It is experimentally established that the absorption properties of (BeO + TiO_2)-ceramics are caused by many factors and, first of all, by its electrical conductivity [18].

The results of studies on the electrophysical properties of (BeO + TiO_2)-ceramics modified by TiO_2 nanoparticles indicate the existence of electric polarization processes and specific relaxation of spatial charges that can accumulate at the boundaries of individual microcrystals. The experimentally observed increase in the conductivity of the synthesized ceramics with an increase in the electric current frequency is explained by the appearance of the current relaxation component accompanied by an increase in the dielectric losses [19, 20].There are very few scientific publications on the study of the effect of TiO_2 nanoparticles on the impedance characteristics of the mechanical mixture of BeO — TiO_2 oxides in the public domain, which may be due to the uniqueness of beryllium production, which requires specialized equipment and special safety conditions when working with powders of BeO. At present, the current production of beryllium oxide ceramics is established in the USA, China and Kazakhstan, so the analysis and updating of knowledge on the results of research on the properties of nanostructured ceramics using this strategically important material seems to be very important.

Thus, the main purpose of the present study is to establish the effect of titanium dioxide nanoparticles on the impedance characteristics of sintered ceramics of 70 wt. % BeO(μm) + TiO_2(μm) + TiO_2(nano) with the introduction of TiO_2 nanoparticles from 0.1 to 2.0 wt. %.

Materials and methods

As a standard sample of two-component ceramics the serial sample of composition BeO + 30 wt. % TiO_2 (mark BT-30) was investigated. To produce nanocomposite ceramics, an annealed beryllium oxide powder with an average crystallite size of 5 μm and a micron powder of titanium dioxide TU 6-10-727-78 with the same particle size were used. From 0.1 to 2.0 wt % of nanodispersed TiO_2 powder was added to the BeO and TiO_2 micropowders. Microphotographs of the particles of the powders used are shown in Figure 1.

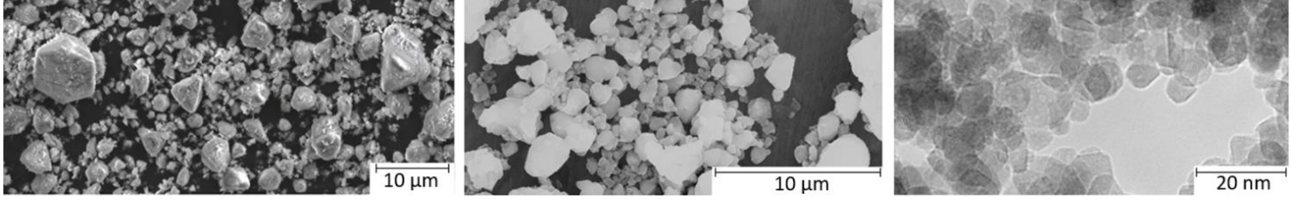

Figure 1. Electronic images of microparticles of beryllium oxide powders, titanium dioxide and nanoparticles of titanium dioxide

Then, the samples were molded by the slip casting method, burned out the bond and sintered the blank at temperatures of 1520 — 1550 ^{0}C with an interval of 10 ^{0}C. Thus, batches of ceramics based on beryllium oxide and titanium dioxide micropowders modified by TiO_2 nanoparticles were obtained with the following composition:

P.0 — BeO + 30 % $TiO_2^{\mu m}$ (BT-30 serial ceramic);
P.1 — BeO + 29,9 % $TiO_2^{\mu m}$+ 0,1 % TiO_2^{nano};
P.2 — BeO + 29,5 % $TiO_2^{\mu m}$+ 0,5 % TiO_2^{nano};
P.3 — BeO + 29,0 % $TiO_2^{\mu m}$+ 1,0 % TiO_2^{nano};
P.4 — BeO + 28,5 % $TiO_2^{\mu m}$+ 1,5 % TiO_2^{nano};
P.5 — BeO + 28,0 % $TiO_2^{\mu m}$+ 2,0 % TiO_2^{nano}.

Particular attention should be paid to the sintering process of the workpiece, which was carried out in a beryllium oxide crucible in a furnace with a graphite heater. The inner part of the crucible was lined with 0.5 mm thick molybdenum sheet, in which technological holes were provided for saturation of the billet with reducing CO gas. The crucible was covered with a beryllium cover with technological holes after the laying of workpieces. The beryllium oxide crucible was installed into the graphite rigging and covered with ballast of sintered oxide-beryllium cast, fraction not more than 10 x 10 mm. After installing graphite tooling with products in the furnace, sintering of the workpiece was carried out.

Measurements of impedance values were carried out on the AgilentE5061B spectrum analyzer designed to measure the total complex resistance (impedance) of composite samples in the frequency range of 100 Hz — 100 MHz. In this instrument model, error minimization and accurate repeatable measurement results are provided by the shielded connector. The inputs of the digital multimeter are also shielded and are optoelectronically isolated from the common case and computer interface circuits. This protection provides a high degree of input isolation, withstanding voltages up to 300 V, which is very important for reducing errors due to ground loops and common mode voltages caused by long wires and floating sources.

At least ten samples from each batch were measured in order to obtain reliable data and statistical values. If the sample had defects in the form of cracks, cavities and pores, the sample was excluded from the experiment. Some samples had relatively high electrical resistance, despite the absence of external defects, most likely there were internal defects, the measurement results of such samples were also excluded. Analysis and deciphering of the obtained data was performed using a personal computer and special software developed on the basis of Excel in the laboratory of antennas and microwave technology, created on the basis of the Department of Radio Engineering of the Institute of Engineering Physics and Radioelectronics of Siberian Federal University (Krasnoyarsk, Russia).

Results and discussion

The results of impedance spectroscopy of a serial sample (P.0) sintered at 1530 ^{0}C without the addition of nanoparticles show that such material is a conductive composite, Figure 2.

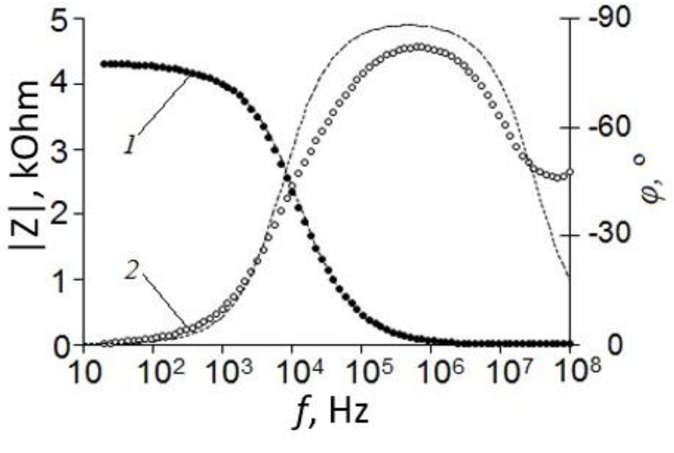

Figure 2. Frequency dependences of impedance modulus |Z| (1) (●) and φ phase angle (2) (○) for serial ceramic samples of composition BeO + 30 wt. %, T = 1530 °C

The values of impedance modulus and phase angle for the sample modified by TiO_2 nanoparticles sintered at 1550 °C are shown in Figure 2. The sample with 0.5 wt % nanoparticles (Fig. 3, a) shows the lowest resistance at low frequencies — 0.38 kOhm; at the maximum frequency of 10^8 Hz — 7.7 Ohm. The phase angle has a single peak of 50° at $5.3 \cdot 10^5$ Hz and gradually decreases with increasing frequency of electric current to -3° at the maximum frequency. When the concentration of TiO_2 nanoparticles is increased up to 1.5 wt % (Figю 3, b), the values of electrical resistance of the sample are observed at low frequencies — 0.45 kOhm and at the maximum frequency of electric current — 8.3 Ohm. The phase angle has exactly the same one peak, which shows itself at the frequency of $4.3 \cdot 10^5$ Hz and is -56°, gradually decreasing with increasing frequency to -4° at the maximum frequency of electric current.

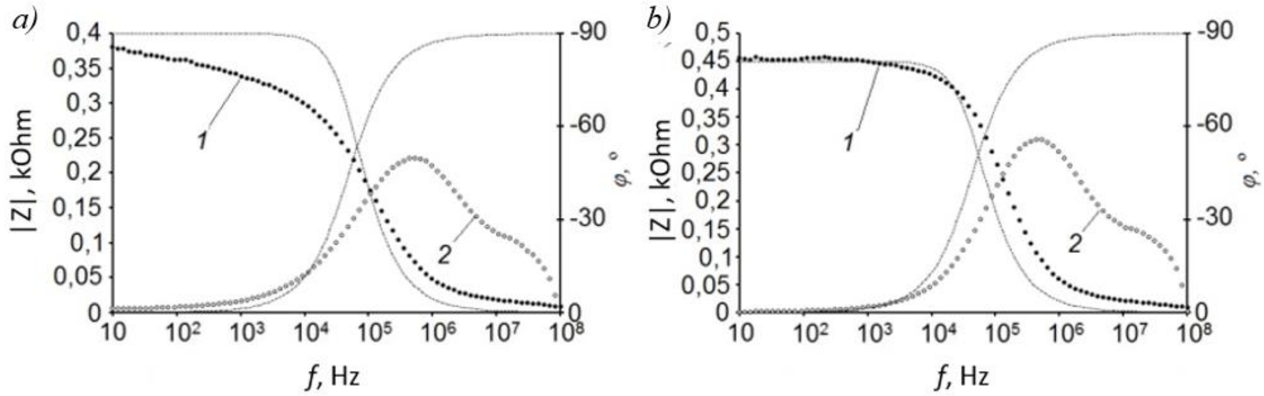

Figure 3. Typical frequency dependences of impedance modulus |Z|(1) (●) and φ phase angle (2) (○), T = 1550 °C: a) (P.2) BeO + 29,5 %$TiO_2^{\mu m}$+ 0,5 %TiO_2^{nano}; b) (P.4) BeO + 28,5 % $TiO_2^{\mu m}$+ 1,5 % TiO_2^{nano}.

The effective component of specific conductivity of serial ceramics (P.0) at low frequencies (up to 10^4 Hz) remains at the level of $2.4 \cdot 10^{-4}$ $Ohm^{-1}m^{-1}$, with further increase in frequency conductivity jumps to the value 0.15 $Ohm^{-1}m^{-1}$ (Fig. 4).

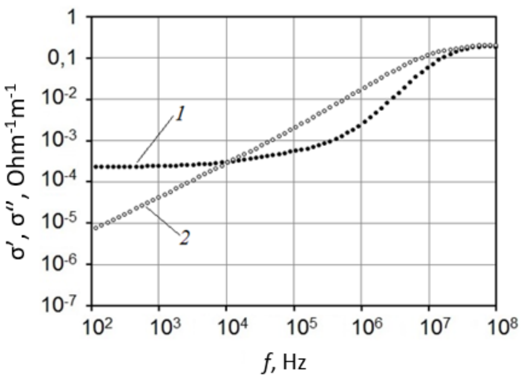

Figure 4. Frequency dependence of actual σ' (1) and imaginary σ' (2) components of specific conductivity of serial ceramics (P.0) of BeO + 30 %$TiO_2^{\mu m}$, T = 1530 °C

Here, the imaginary component of the specific conductivity increases linearly over the entire investigated frequency range, which corresponds to the real component at frequencies above $3 \cdot 10^7$ Hz.

By increasing the sintering temperature to 1550 °C (Fig. 5), the conductivity curves depending on the content of TiO_2 nanoparticles are parallel to each other in the frequency range from 10 to 10^5 Hz. The minimum conductivity value at this site is σ'(1.0 %) = $5.5 \cdot 10^{-3}$, the maximum σ'(0.1 %) = $4.8 \cdot 10^{-2}$ $Ohm^{-1}m^{-1}$. With increase of frequency of electric field the specific conductivity on all samples sharply increases, at the maximum frequency of 10^8 Hz conductivity curves practically coincide, here maximum value σ'(0,5 %) = 1,36 $Ohm^{-1}m^{-1}$.

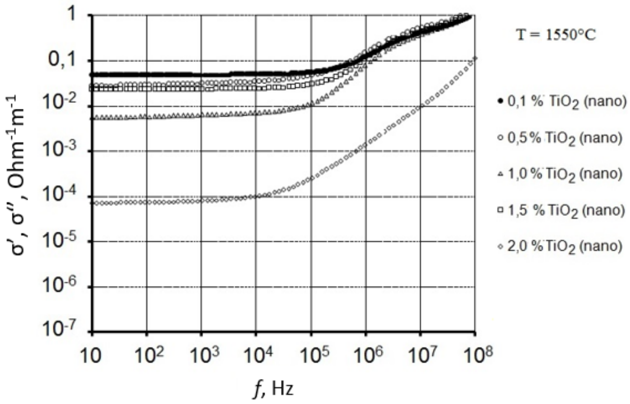

Figure 5. Frequency dependence of actual σ' component of specific conductivity as a function of TiO_2 nanoparticles content, T = 1550 °C (P.1 — P.5)

The sintering temperature, which provides stable high conductivity in the range of electric field frequencies from 10 to 10^8 Hz, is 1530 — 1550 °C. The conductivity mechanism can be explained by the fact that during sintering of ceramics the TiO_2 nanoparticles are pushed to the surface of micron granules (i.e., to the intercrystalline interlayers). Thus, the frequency dependence of the specific conductivity depending on the nanoparticle content observed in Figure 5 can be explained by the fact that the conductivity follows a random grid of interlayers between the crystals, as shown in Figure 8a. Some layers of neighboring crystals may not interact, hence the finite resistance and jumping mechanism of conductivity from one layer to another (between the layers) appear. As the concentration of titanium dioxide nanoparticles increases up to 2.0 %, they begin to adhere to each other or to titanium oxide microparticles inside the crystal and do not go into the intergranular layers, so that the material becomes a dielectric.

Figure 6 shows the curves of change in the values of the real and imaginary components of dielectric permittivity, the tangent of the angle of dielectric losses depending on the frequency of electric current in a sample of serial ceramics (P.0).

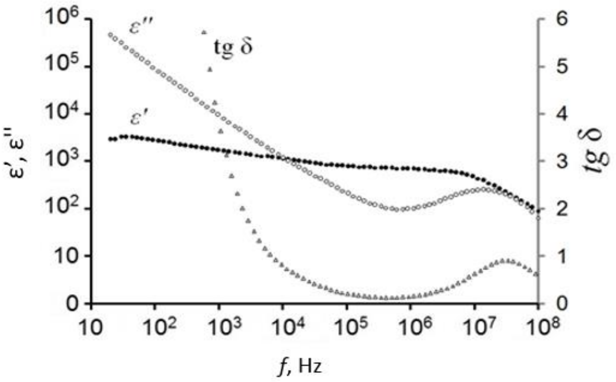

Figure 6. Variation curves of values of the actual and imaginary components of dielectric permittivity, dissipation factor for the factory sample composition: BeO + 30 % $TiO_2^{\mu m}$, T = 1530 °C (P.0)

For this sample at low frequencies both components of dielectric permittivity have anomalously high values. With increasing frequency of electric field, we observe uniform fall of values ε' and ε". For ε' after 10^7 Hz there is a sharper drop to ~ 80 at 10^8 Hz. The imaginary component ε" decreases more rapidly with increasing frequency, at $8{\cdot}10^5$ Hz there is some rise and again a drop of value ε" ~ 40 at maximum frequency.

Tangent of dielectric loss angle also has anomalously high values at low frequencies and sharply decreases with frequency increase. At frequency 10^4 Hz tgδ = 1,0, the minimum value of tgδ = 0,1 is observed at frequency $9{\cdot}10^5$ Hz, which increases with frequency and has a peak tgδ = 1,0 at frequency $5{,}5{\cdot}10^7$ Hz. At the 10^8 Hz maximum frequency tgδ = 0.63.

The maximum dielectric losses are observed in the sample of nanocomposite ceramics sintered at 1550 °C (Fig. 7).

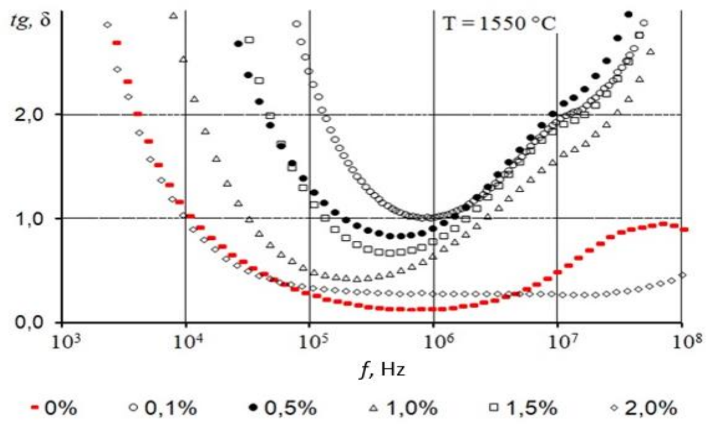

Figure 7. Frequency dependence of the dissipation factor on the content of TiO_2 nanoparticles, T = 1550 °C (P.1 — P.5)

Thus, increasing the sintering temperature of ceramics containing nanoparticles in the range (0.1-1.5) wt % leads to an increase in conductivity, dielectric permittivity, and, most importantly, the tangent of the dielectric loss angle increases.

The increase in dielectric losses observed in Figure 7 can be explained by the fact that the nanoparticles in the investigated ceramics are located on the crystal surface, where the charges can also shift to the opposite crystal boundaries, which leads to the appearance of intracluster current. Such displacement of charges can be accompanied by appearance of additional ceramic polarizability in its volume and growth of dielectric permittivity mainly in the region of low frequencies. But as the electric field frequency increases, the charges do not have time to shift to the cluster boundary, they lag behind the external field in phase, which is the cause of dielectric losses.

The mechanism of electrical conductivity of such ceramics can be explained in terms of a composite material in which the dielectric does not participate in current transfer after the p_c percolation threshold [21]. Percolation theory, from Latin percolatio is a mathematical theory that is used in physics to study processes occurring in heterogeneous media with random properties, but fixed in space and unchanged in time. Thus, it means that, under any conditions, the electrical conductivity of the filler is much higher than that of the matrix and no interfacial layers with other properties are formed in such a composite. When the concentration p of the filler increases (in our case it is TiO_2), the effective conductivity increases according to:

$$\sigma(p) = \sigma_1 (p - p_c)^t, \quad (1)$$

where t is the critical conductivity index; σ_1 is the specific conductivity of the dispersed conductive phase. This formula is applicable to describe the electrical conductivity of the system after the percolation threshold $p \geq pc$. The following complementary laws of degrees can be introduced into formula (1):

$$\sigma(p_c) = \sigma_1 h^s, \text{ at } p \approx p_c; \quad (2)$$

$$\sigma(p) = \sigma_2 (p_c - p)^{-q} = \sigma_1 h (p_c - p)^{-q}, \text{ at } p < p_c, \quad (3)$$

where s and q are critical indexes, $h = \sigma_2 / \sigma_1$.

The increase in σ with increasing p by (3) is associated with a gradual increase in the size of metal clusters and the area of dielectric interlayers between neighboring clusters. Immediately in the region of pc the power laws (1) and (3) are disturbed and by (2) pass into each other. If the disperse phase is randomly distributed over the volume, then up to the percolation threshold (p < pc) the dielectric matrix interlayers, whose local resistance is much greater than that of the disperse phase particles, participate in charge transfer through the sample. Thus, in the region of the percolation threshold at direct current, dielectric interlayers have the most significant effect on the electrical characteristics of the entire composite.

On alternating current, in addition to the resistance of the matrix interlayers, it is necessary to take into account the capacitances of the “capacitors” formed by the particles (cluster sites) of the electrically conducting phase and the dielectric matrix interlayers.

A schematic representation of such a composite, up to the percolation threshold is shown in Figure 8, a.

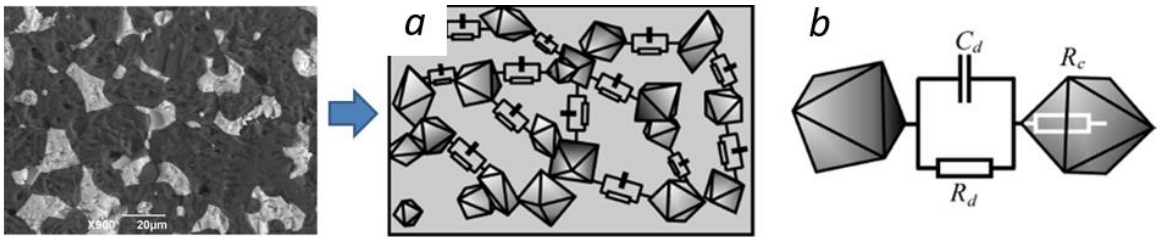

Figure 8. Schematic representation of the composite material structure [21] (in the inset on the left is an electronic image of the microstructure of a ceramic sample of composition P.3): a) up to the flow threshold; b) equivalent substitution scheme

Figure 8, a shows the resistive-capacitive coupling between the clusters and the particles of the electrically conducting phase by parallel RC circuits.

In composites at $p < p_c$ the infinite cluster is not formed and the equivalent circuit of Figure 8 b must contain two resistors connected in series. The first resistor corresponds to the resistance *Rc* of clusters and particles of the electrically conductive phase. The second resistor takes into account the resistance of dielectric matrix interlayers *Rd*, and the resistor *Rd* is shunted by a capacitor *Cd*, the capacity of which corresponds to the capacitance of matrix interlayers.

To analyze the resistive-capacitive properties of the studied substances and to understand the electrophysical processes occurring in them, we used the method of constructing suitable electrical circuits impedance of which agrees with the experiment. For these samples of ceramics using a special program *EISA-analizer* the most suitable equivalent circuits were selected, which are shown in Figure 9 a, b.

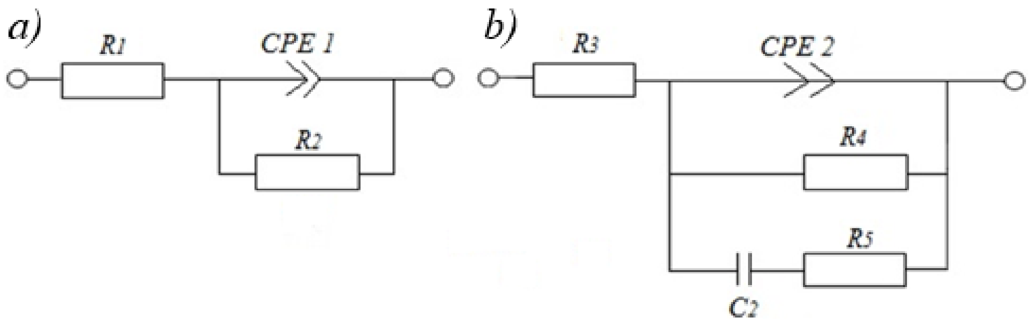

a — sample of composition P.1; b — sample of composition P.0

Figure 9. Equivalent schemes for samples

As can be seen, both circuits contain the usual radio engineering elements R-resistance and C-capacitance. In these circuits there is a linearly dependent parameter, an artificial constant phase element (CPE), which to some extent reflects the electrical properties of a variety of structurally heterogeneous materials. The impedance (Z_{CPE}) of this element is written in the following form:

$$Z_{CPE} = \frac{1}{A(i\omega)^n} = \frac{1}{A\omega^n}\left[\cos\left(\eta\frac{\pi}{2}\right) - i\sin\left(\eta\frac{\pi}{2}\right)\right] \tag{4}$$

where *A* is the numerical multiplier, *ω* is the circular frequency, *i* is the imaginary unit, and *η* is the exponent determining the nature of the impedance frequency dependence ($-1 \le \eta \le 1$). The *CPE* element has both a real and imaginary component. For integer values of η = 1, 0, -1 the *CPE* element degenerates to the usual *C*, *R*, *L* elements. Fractional values of the index of degree η < 1 formally characterize the cluster structure of the material.

The simplest electrical circuit for TiO_2 nano-added ceramics Figure 9a contains only three elements: resistance R_1 = 2.9 Ohm, R_2 = 827 Ohm and element CPE_1 with numerical multiplier $A_0 = 5.32 \cdot 10^{-9}$ and exponent close to unity η = 0.92. The smaller number of resistances in the circuit for the nanophase sample, explains the increase in specific conductivity and dielectric losses with increasing frequency of electric current. It can be noted that the resistance R_2 almost coincides in magnitude with the low-frequency impedance of this ceramic |Z| = 830 Ohm and naturally simulates the static resistance of ceramics. Resistance R_1 = 2.9 Ohm in the region of radio frequencies remains virtually unnoticed, but with increasing frequency, when the impedance of the sample decreases, this resistance makes a tangible contribution to the formation of the impedance spectrum. In particular, it is this resistance in the region of high and possibly ultra high frequencies leads to the observed in the impedance spectrum reduction of the phase of the AC current flowing through the sample. The results of numerical approximation of the experimentally measured impedance spectrum of these ceramics with the equivalent circuit are shown in Figure 10a with solid lines. As can be seen the coincidence of the calculation with the experiment is quite satisfactory.

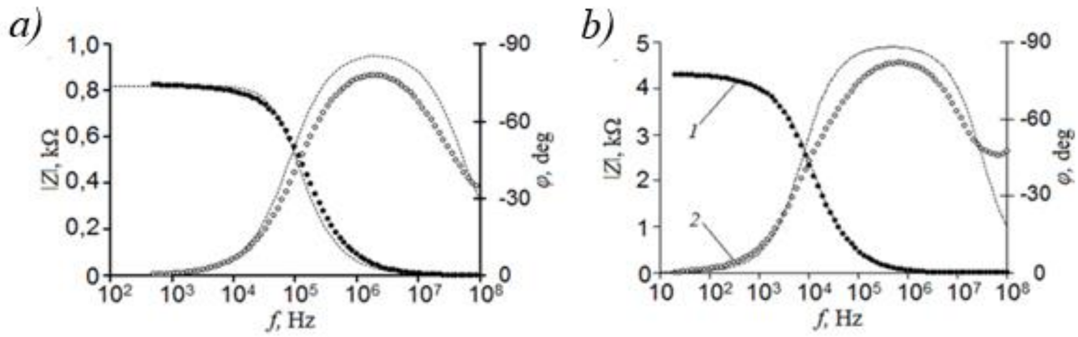

a — sample of composition P.1; b — sample of composition P.0.

Figure 10. Frequency dependences of the impedance modulus Z (1) and phase angle φ (2) (white markers). The results of numerical approximation using the equivalent scheme are shown by solid lines.

For a sample of ceramics with micropowder TiO_2, the frequency dependence of impedance is shown in Figure 10b, and the equivalent circuit is shown in Figure 9 b. As can be seen this scheme is more complex and in addition to the element CPE_2 contains two parallel circuits one of which consists of a resistance $R_4 = 4300\ Ohm$ simulating the static resistance of ceramics. The second circuit is formed by series elements $C_2 = 2{,}9 \cdot 10^{-8}\ F$ and *R5 = 4 Ohm* which form impedance characteristics in the middle frequencies. The CPE_2 element has a numerical multiplier $A_0 = 2.9 \cdot 10^{-8}$ and power factor *n* = 0.72. This power factor means that the CPE_2 element can be treated as a frequency-dependent capacitance and simultaneously as a frequency-dependent resistance. Resistor R_3, as for the previous sample, serves to simulate high-frequency electrical losses. To simulate impedance in the decimeter and centimeter wavelength range it may be necessary to introduce additional elements. Thus, the different ratio in the ceramic of TiO_2 nanoparticles and the degree of its reduction allow to significantly reduce the static impedance, thereby improving the conductivity and regulating the magnitude of electromagnetic radiation absorption by such ceramics.

Conclusion

Analyzing the experimental results obtained in the work, we can make the following conclusions:

– It is established that the introduction of nanoparticles TiO_2 in an amount (0.5 — 1.5) wt. % in the composition of ($BeO + TiO_2$)-ceramics significantly reduces its static electrical resistance in comparison with the serial sample. So at high frequencies, ~ 10^7 Hz, resistance decreases three times (from 0.024 to 0.008 kOhm), with the introduction of nano-particles (0.5 — 1.5) mass % and sintering temperature of ceramics 1530 — 1550 °C. The sample made of micropowders at the same frequency has an electrical resistance of 0.036 kOhm.

– It is established that the specific conductivity of ceramics modified by TiO_2 nanoparticles (0.5 — 1.5) mass % at high frequencies ~ 10^7 Hz increases from 0.3 to 1.4 $Ohm^{-1}m^{-1}$ in samples obtained in the temperature range of sintering ceramics 1530 — 1550 °C. The conductivity of the sample made of micropowders at the same frequency is 0.68 $Ohm^{-1}m^{-1}$. The increase in sintering temperature is associated with the formation of new phases.

– The addition of nanoparticles TiO_2 (0,5 — 1,5) wt. %, in composition of ($BeO + TiO_2$)-ceramics essentially increases dielectric losses of the sample sintered in the interval of temperatures 1530 — 1550 °C. Values of real and imaginary components of dielectric permittivity of such ceramics $\varepsilon' = 58$ — 120, $\varepsilon'' = 52$ — 314. For the sample made of micropowders at the same frequency $\varepsilon' = 60$, $\varepsilon'' = 40$. The tangent angle of dielectric losses in nanocomposite ceramics is twice as high.

– It is shown that the ceramic samples have electrical conductivity, which increases in proportion to the angular frequency with a fractional index of degree. This allowed us to identify the conductivity of the sample with microparticles as a jump-type conductivity. In the sample with TiO_2 nanoparticles the conductivity dispersion is not detected, and the observed in the experiment non-monotone growth of conductivity with increasing frequency is explained by the appearance of the current relaxation component accompanied by an increase in dielectric losses.

Acknowledgments

This research was funded by the Science Committee of the Ministry of Education and Science of the Republic of Kazakhstan (Grant No. AP09058686).

References

1 Бухарин Е.Н. Объемные поглотители СВЧ-энергии в конструкциях современных электровакуумных СВЧ-приборов и измерительных устройств / Е.Н. Бухарин, Е.Н. Ильина // Радиотехника. — 2014. — Т. 15. — № 11. — С. 57–64.

2 Lu G. Dielectric and microwave absorption properties of KNN/Al2O3 composite ceramics / G.Lu, Z. Wancheng, L.Fa, Z. Dongmei, W. Jie // Ceramics International. — 2017. — V. 43. — Is. 15. — P. 12731-12735.

3 Belyaev B.A. Study of electrophysical properties of cation-substitution ceramic of barium hexa-aluminate by impedance spectroscopy / B.A. Belyaev, N.A. Drokin, V.A. Poluboyarinov // FTT. — 2018. — Vol. 60(2). — P. 266-275.

4 Kiiko V.S. Ceramics Based on Beryllium Oxide: Preparation, Physicochemical Properties, and Application / V.S. Kiiko, Yu.N. Makurin, A.L. Ivanovskii // UrO RAN, Ekaterinburg. — 2006.

5 Дрокин Н.А. Электрофизические свойства керамики БТ–30 / Н.А. Дрокин, В.С. Кийко, А.В. Павлов, А.И. Малкин // Новые огнеупоры. — 2020. — № 6. — С. 56–63.

6 Щербина А. Изделия из керамики на основе оксида алюминия, нитрида алюминия и оксида бериллия производства АО «Тестприбор» ООО «Медиа КиТ», Санкт-Петербург / А. Щербина, Л. Федорович // Силовая электроника. — 2019. — № 4. — С. 68–70.

7 Беляев Р.А. Окись бериллия / Р.А. Беляев // Атомиздат. — 1980. — С. 221.

8 Вайспапир В.Я. Бериллиевая керамика для современных областей техники / В.Я. Вайспапир, В.С. Кийко // Вестн. воздушно-космической обороны. — 2018. — № 1 (17). — С. 59–69.

9 Zdorovets V. Study of change in beryllium oxide strength properties as a result of irradiation with heavy ions / V. Zdorovets, A.L. Kozlovskiy, D.B. Borgekov, D.I. Shlimas // Eurasian Journal of Physics and Functional Materials. — 2021. — Vol. 5(3). — P. 192-199.

10 Akishin G.P. Thermal conductivity of beryllium oxide ceramic / G.P. Akishin, S.K. Turnaev, V.Ya. Vaispapir, M.A. Gorbunova, Yu.N. Makurin, V.S. Kiiko, A.L. Ivanovskii. // Refractories and Industrial Ceramics. — 2009. — Vol. 5050. — P. 465-468.

11 Kiiko V.S. Fabrication, physicochemical properties, and transmission of microwave radiation by BeO-based ceramics / V.S. Kiiko, S.N. Shabunin, Yu.N. Makurin // Ogneup. Tekh. Keram. — 2004. — No. 10. — P. 8-17.

12 Kiiko V.S. Transparent beryllia ceramics for laser technology and ionizing radiation dosimetry / V.S. Kiiko // Refractories and Industrial Ceramics. — 2004. — Vol. 45, No 4. — P. 266-272.

13 Акишин Г.П. Свойства оксидной бериллиевой керамики / Г.П. Акишин, С.К. Турнаев, В.Я. Вайспапир [и др.] // Новые огнеупоры. — 2010. — № 10. — С. 42–47.

14 Кийко В.С. Теплопроводность и перспективы применения BeO-керамики в электронной технике / В.С. Кийко, В.Я. Вайспапир // Стекло и керамика. — 2014. — № 11. — С. 12–16.

15 Ивановский А.Л. Электронная структура и свойства оксида бериллия / А.Л. Ивановский, И.Р. Шеин, Ю.Н. Макурин, В.С. Кийко, М.А. Горбунова // Неорганические материалы. — 2009. — Т. 45, № 3. — С. 263–275.

16 Drokin N.A. BT-30 ceramic electrophysical properties / N.A. Drokin, V.S. Kiiko, A.V. Pavlov, A.I. Malkin // Refractories and Industrial Ceramics. — 2020. — Vol. 61, No. 3. — P. 341-348.

17 Лепешев А.А. Особенности получения и исследование электрофизических характеристик ($BeO+TiO_2$)-керамики методом импедансной спектроскопии // А.А. Лепешев, А.В. Павлов, Н.А. Дрокин, А.И. Малкин, В.С. Кийко // Новые огнеупоры. — 2019. — № 6. — С. 55–63.

18 Кийко В.С. Керамика на основе оксида бериллия: получение, физико-химические свойства и применение //В.С. Кийко, Ю.Н. Макурин, А.Л. Ивановский // Екатеринбург: УрО РАН, 2006. — С. 440.

19 Кийко В.С. Микроструктура и электропроводность композиционной ($BeO+TiO_2$)-керамики // В.С. Кийко, М.А.Горбунова, Ю.Н. Макурин // Новые огнеупоры. — 2007. — № 11. — С. 68–74.

20 Кийко В.С. Влияние добавок диоксида титана на физико-химические и люминесцентные свойства бериллиевой керамики / В.С. Кийко // Неорганические материалы. — 1994. — Т. 30, № 5. — С. 688–693.

21 Поклонский Н.А. Основы импедансной спектроскопии композитов: курс лекций / Н.А. Поклонский, Н.И. Горбачук. — Минск: Белорус. гос. ун-т, 2005. — С. 83–90.

А.В. Павлов, А.М. Жилкашинова, С.С. Герт, Н.М. Магазов, Ж.С. Тұрар, А.Б. Набиолдина

Титан диоксиді микро және нанобөлшектері қосылған бериллий керамикасының электрофизикалық қасиеттерін зерттеу

Мақалада микроұнтақтардан жасалған оксид-бериллий керамикасының ($BeO + TiO_2$) электрофизикалық қасиеттеріне 0,1-2,0 масс% аралығындағы TiO_2 наноөлшемді бөлшектердің қоспаларының әсерін зерттеу нәтижелері келтірілген. Толық кешенді кедергі (импеданс) әдісімен 30 масс% мөлшерінде TiO_2 микро және нанобөлшектерімен модификацияланған синтезделген керамиканың 100 Гц — 100 МГц электр тогының жиілік диапазонында электрофизикалық сипаттамалары зерттелді. Тотықсыздану атмосферасында термиялық өңдеуден кейін TiO_2 қоспасын BeO-керамикаға енгізу электр өткізгіштігінің айтарлықтай жоғарылауымен және жиіліктің кең диапазонында электромагниттік сәулеленуді сіңіру қабілетімен бірге жүретіні белгілі. Зерттеу нәтижелері бойынша TiO_2 нанобөлшектерінің ($BeO + TiO_2$)-керамикасына енгізу оның статикалық электр кедергісін сериялық үлгімен салыстырғанда едәуір төмендететіні анықталды, ал мұндай керамиканың нақты өткізгіштігі ~ 10^7 Гц жоғары жиілікте айтарлықтай артады. TiO_2 нанобөлшектерін енгізу 1530—1550 °C температура аралығында агломерацияланған үлгінің диэлектрлік шығынын едәуір арттырады. Мұндай керамиканың диэлектрлік өткізгіштігінің нақты және жорамал компоненттерінің мәні және диэлектрлік жоғалту бұрышының тангенсі БТ-30 (Б-бериллий, Т-титан) сериялық үлгімен салыстырғанда екі есе жоғары. Зерттеу нәтижелері сирек кездесетін және стратегиялық маңызды материалмен — бериллий оксидімен және оның негізінде жаңа наноқұрылымдарды синтездеу мүмкіндігімен эксперименттеуге байланысты болып табылады.

Кілт сөздер: диэлектрлік өткізгіштік, өткізгіштік, электр тогының жиілігі, кедергі, нанобөлшектер, бериллий оксиді, титан диоксиді.

А.В. Павлов, А.М. Жилкашинова, С.С. Герт, Н.М. Магазов, Ж.С. Тұрар, А.Б. Набиолдина

Исследование электрофизических свойств бериллиевой керамики с добавкой микро- и наночастиц диоксида титана

В статье представлены результаты исследования влияния добавок наноразмерных частиц TiO_2 в интервале 0,1–2,0 масс. % на электрофизические свойства оксидно-бериллиевой керамики состава ($BeO+TiO_2$), изготовленной из микропорошков. Методом полного комплексного сопротивления (импеданса) исследованы электрофизические характеристики синтезированной керамики, модифицированной микро- и наночастицами TiO_2 в количестве 30 масс. % в диапазоне частот электрического тока 100 Гц–100 МГц. Известно, что введение в BeO-керамику добавки TiO_2 после термообработки в восстановительной атмосфере сопровождается значительным увеличением электропроводности и способностью поглощать электромагнитное излучение в широком диапазоне частот. По результатам исследований установлено, что введение в состав ($BeO+TiO_2$)-керамики наночастиц TiO_2 значительно снижает ее статическое электросопротивление по сравнению с серийным образцом, а удельная проводимость такой керамики значительно возрастает на высоких частотах ~ 10^7 Гц. Добавка наночастиц TiO_2 существенно увеличивает диэлектрические потери образца, спеченного в интервале температур 1530–1550 °C. Значения действительной и мнимой компоненты диэлектрической проницаемости такой керамики и тангенс угла диэлектрических потерь выше в два раза в сравнении с серийным образцом БТ–30 (Б — бериллий, Т — титан). Полученные результаты исследований являются уникальными в своем роде, что обусловлено экспериментом с редким и стратегически важным материалом — оксидом бериллия и возможностью синтеза новых наноструктур на его основе.

Ключевые слова: диэлектрическая проницаемость, проводимость, частота электрического тока, импеданс, наночастицы, оксид бериллия, диоксид титана.

References

1 Bukharin, E.N., & Ilina, E.N. (2014). Obemnye poglotiteli SVCh-energii v konstruktsiiakh sovremennykh elektrovakuumnykh SVCh-priborov i izmeritelnykh ustroistv [Volumetric absorbers of microwave energy in the designs of modern electrovacuum microwave devices and measuring devices]. *Radiotekhnika – Radio engineering* 15(11), 57–64 [in Russian].

2 Lu, G., Wancheng, Z., Fa, L., Dongmei, Z., & Jie, W. (2017). Dielectric and microwave absorption properties of KNN/Al2O3 composite ceramics. *Ceramics International, 43*(15), 12731-12735.

3 Belyaev, B.A. Drokin, N.A., & Poluboyarinov, V.A. (2018). Study of electrophysical properties of cation-substitution ceramic of barium hexa-aluminate by impedance spectroscopy. *FTT*, *60*(2), 266-275.

4 Kiiko, V.S. Makurin, Yu.N., Ivanovskii, A.L. (2006). Ceramics Based on Beryllium Oxide: Preparation, Physicochemical Properties, and Application. *UrO RAN*, Ekaterinburg.

5 Drokin, N.A., Kiiko, V.S., Pavlov, A.V., & Malkin, A.I. (2020). Elektrofizicheskie svoistva keramiki BT–30 [Electrophysical properties of BT-30 ceramics]. *Novye ogneupory — New refractories*, *6*, 56–63 [in Russian].

6 Sherbina, A. & Fedorovich, L. (2019). Izdeliia iz keramiki na osnove oksida aliuminiia, nitrida aliuminiia i oksida berilliia proizvodstva AO «Testpribor» [Ceramic products based on aluminum oxide, aluminum nitride and beryllium oxide produced by “Testpribor” JSC]. LLC «Media KiT». *Silovaia elektronika — Power electronics*, *4*, 68-70. Saint Petersburg [in Russian].

7 Belyaev, R.A. (1980). Okis berilliia [Beryllium oxide]. *Atomizdat*, 221 [in Russian].

8 Vaispapir, V.Ya. & Kiiko, V.S. (2018). Berillievaia keramika dlia sovremennykh oblastei tekhniki [Beryllium ceramics for modern engineering fields]. *Vestnik vozdushno-kosmicheskoi oborony — Bulletin of aerospace defense*, *1*(17), 59–69 [in Russian].

9 Zdorovets, V., Kozlovskiy, A.L., Borgekov, D.B., & Shlimas, D.I. (2021). Study of change in beryllium oxide strength properties as a result of irradiation with heavy ions. *Eurasian Journal of Physics and Functional Materials*, *5*(3), 192-199.

10 Akishin, G.P., Turnaev, S.K., Vaispapir, V.Ya., Gorbunova, M.A., Makurin, Yu.N., Kiiko, V.S., & Ivanovskii, A.L. (2009). Thermal conductivity of beryllium oxide ceramic. *Refractories and Industrial Ceramics*, *5050*, 465-468.

11 Kiiko, V.S., Shabunin, S.N., & Makurin, Yu.N. (2004). Fabrication, physicochemical properties, and transmission of microwave radiation by BeO-based ceramics. *Ogneup. Tekh. Keram*, *10*, 8-17.

12 Kiiko, V.S. (2004). Transparent beryllia ceramics for laser technology and ionizing radiation dosimetry. *Refractories and Industrial Ceramics*, *45*(4), 266-272.

13 Akishin, G.P., Turnaev, S.K., & Vaispapir, V.Ya. (2010). Svoistva oksidnoi berillievoi keramiki [Properties of oxide beryllium ceramics]. *Novye ogneupory — New refractories, 10*, 42–47 [in Russian].

14 Kiiko, V.S., & Vaispapir, V.Ya. (2014). Teploprovodnost i perspektivy primeneniia BeO-keramiki v elektronnoi tekhnike [Thermal conductivity and prospects of application of BeO-ceramics in electronic engineering]. *Steklo i keramika — Glass and ceramics*, *11*, 12–16 [in Russian].

15 Ivanovskii A.L., Shein, I.R., Makurin, Yu.N., Kiiko, V.S., & Gorbunova, M.A. (2009). Elektronnaia struktura i svoistva oksida berilliia [Electronic structure and properties of beryllium oxide]. *Neorganicheskie materialy — Inorganic materials, 45*(3), 263–275 [in Russian].

16 Drokin, N.A., Kiiko, V.S., Pavlov, A.V., & Malkin, A.I. (2020). BT-30 ceramic electrophysical properties. *Refractories and Industrial Ceramics*, *61*(3), 341-348.

17 Lepeshev, A.A., Pavlov, A.V., Drokin, N.A., Malkin, A.I., & Kiiko, V.S. (2019). Osobennosti polucheniia i issledovanie elektrofizicheskikh kharakteristik (BeO+TiO_2)-keramiki metodom impedansnoi spektroskopii [Peculiarities of obtaining and investigation of electrophysical characteristics of (BeO + TiO_2)-ceramics by impedance spectroscopy]. *Novye ogneupory — New refractories, 6*, 55–63 [in Russian].

18 Kiiko, V.S., Makurin, Yu.N., & Ivanovskii, A.L. (2006). Keramika na osnove oksida berilliia: poluchenie, fiziko-khimicheskie svoistva i primenenie [Ceramics based on beryllium oxide: preparation, physical and chemical properties and application]. *Ekaterinburg: UrO RAN*, 440 [in Russian].

19 Kiiko, V.S., Gorbunova, M.A., & Makurin, Yu.N. (2007). Mikrostruktura i elektroprovodnost kompozitsionnoi (BeO+TiO_2)-keramiki [Microstructure and electrical conductivity of composite (BeO + TiO_2)-ceramics]. *Novye ogneupory — New refractories, 11*, 68–74 [in Russian].

20 Kiiko, V.S. (1994). Vliianie dobavok dioksida titana na fiziko-khimicheskie i liuminestsentnye svoistva berillievoi keramiki [Influence of additives of titanium dioxide on physico-chemical and luminescent properties of beryllium ceramics]. *Neorganicheskie materialy — Inorganic Materials*, *5*, 30, 688–693 [in Russian].

21 Poklonskii, N.A., & Gorbachuk, N.I. (2005). Osnovy impedansnoi spektroskopii kompozitov: kurs lektsii [Fundamentals of impedance spectroscopy of composites: a course of lectures]. *Minsk: Belorusskii gosudarstvennyi universitet*, 83–90 [in Russian].